



Numerical modelling of flow characteristics over sharp crested triangular hump



Ebrahim Hamid Hussein Al-Qadami^{a,*}, Abdurrahman Sa'id Abdurrahman^a,
Zahiraniza Mustaffa^a, Khamaruzaman Wan Yusof^a, M.A. Malek^b, Aminuddin Ab Ghani^c

^a Department of Civil and Environmental Engineering, Universiti Teknologi PETRONAS, Seri Iskandar, Malaysia

^b Institute of Sustainable Energy (ISE) Universiti Tenaga Nasional Selangor, Malaysia

^c River Engineering and Urban Drainage Research Center Universiti Sains Malaysia Pulau Pinang, Malaysia

ARTICLE INFO

Keywords:

Crump weirs
Flow-3D
Flow over hump
Numerical simulation

ABSTRACT

Research findings have shown that accurate estimation of performance and water surface profiles in hydraulic structures are cumbersome and time-consuming. Furthermore, investigating hydraulic variables experimentally required more money to conduct the field tests and to find the needed equipment. Additionally, laboratory measurements of the hydraulic parameters are not accurate when compared with numerical simulation results. Therefore, numerical simulation of hydraulic problems such as flow over hump using computational fluid dynamics (CFD) science is a great alternative for laboratory tests. In this study, the flow properties of a sharp crested triangular weir of dimension $50 \times 30 \times 7 \text{ cm}^3$ was modelled numerically using Flow 3D and validated using laboratory experiments. Results showed that the software modelled the hydraulic parameters such as the flow surface elevation, Froudes number, velocity and water depths through the triangular hump with a greater degree of performance and accuracy (minimum variations between 4% and 5%). Flow 3D was therefore recommended as a useful tool to predict and investigate the flow behaviour at upstream and downstream of the weirs as well as in different hydraulic structure. In addition, similar modelling with other turbulence models within the software can be considered a strong scientific contribution to the field and is therefore highly recommended for future studies.

Introduction

In open channels, the most common hydraulic structures used for flow discharge measurements are the weirs because of their accuracy, simplicity, and ease of design and construction [1,2]. Their main functions include managing water levels at upstream and downstream as well as measuring flow discharge and channel stabilizations [3]. In addition, they have different engineering applications in the laboratory and field especially in safety, for example in discharging excess water from rivers and dams during flood times. Weirs can be categorized into different types based on their geometry and design. These include broad-crest, sharp-crested, narrow crested, and ogee-shaped weirs. However, based on opening shape, weirs can be classified into 3 main types namely, rectangular, triangular and trapezoidal weirs [4]. Short-crested triangular weirs or crump weirs are among the special types of broad-crested with back face slope of 1:5 and front face slope of 1:2 [5]. In these types of weirs, accurate estimation of performance and water surface profiles are sometimes cumbersome and time-consuming. Complex problems are

therefore required to be solved using accurate and simplified numerical techniques that have been validated with experimental results [6,7].

Nowadays, solving engineering problems by numerical simulation approach have been increased especially with the huge improvement in the capacity and ability of computer processing powers [8]. However, validation of the numerical solution experimentally is required to ensure that the results of modelling are accurate enough. In terms of fluid numerical simulation, finite volume method and finite element method are used to solve the fluid governing equations which are continuity and NavierStokes equations in addition to turbulence models [9–12].

Computational fluid dynamics (CFD) had been reported among the numerical simulation techniques used to solve fluid flow problems [13]. In this field, many commercial and open source codes have been developed for numerical simulations. Among the most popular ones are Fluent, Flow-3D and Star CCM+, while open-FOAM code is an example of an open source CFD code [14]. Flow-3D software uses the finite volume method (FVM) to solve the governing equations and different turbulent models are available including two-equation k-ε model, re-normalized

* Corresponding author.

E-mail address: ialgodami@gmail.com (E.H.H. Al-Qadami).

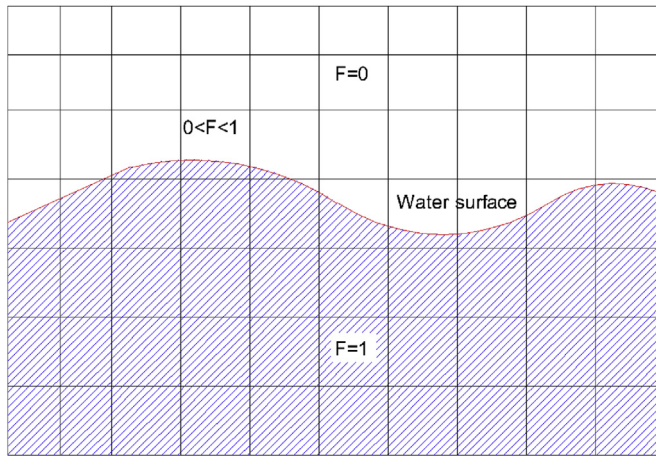


Fig. 1. Empty and fully cells water fraction (F).

group (RNG) model, two-equation, k-w model and one-equation turbulent energy model [15–17]. However, k-ε and (RNG) models are the most advanced equations commonly used for fluid engineering [18–20]. Most previous studies employed the use of experimental methods and some time with simplified theoretical expressions to validate problems in crested weirs. However, developing a properly validated model using a numerical technique can be highly applicable in studying and characterizing fluid properties and can minimize the frequent use of expensive and time-consuming experimental methods. This study, therefore, analyzed the flow characteristics through sharp-crested rectangular weir of dimension 50 cm × 30 cm × 7 cm using laboratory experiments and validated numerically using Flow-3D.

Theory and governing equations

Recently, numerical solutions have become a means of solving complicated problems that are difficult or expensive to achieve in the laboratory. In this study, the commercial CFD software, Flow 3D which applies the fluid equations of motion to solve the non-linear, transient, second-order differential equations to describe the motion of the fluid was used. The governing equations involved include the continuity Equations (1) and (2) and Reynolds-averaged Navier-Stokes Equations (3)–(6) [21].

$$\frac{\partial \rho}{\partial t} + \Delta \cdot (\rho v) = 0 \tag{1}$$

where,



Fig. 2. Flow over hump during lab experiment.

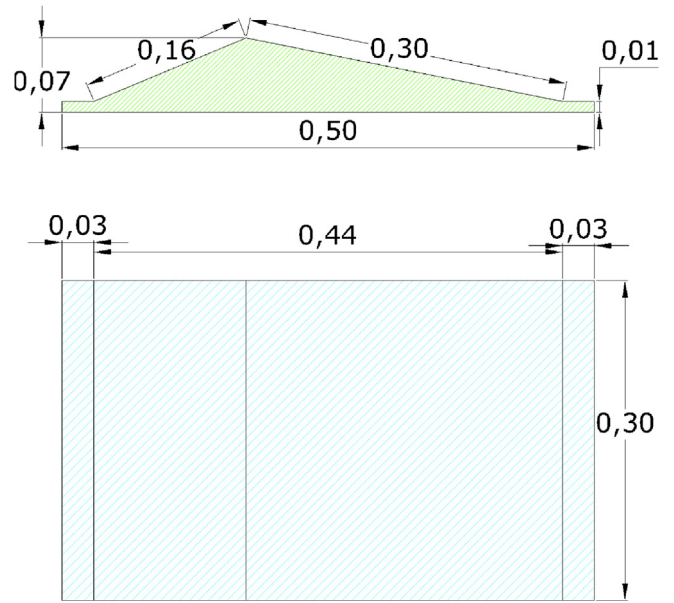


Fig. 3. Hump geometry and dimensions.

$$\Delta \cdot (\rho v) = \frac{\partial \rho u}{\partial x} + \frac{\partial \rho v}{\partial y} + \frac{\partial \rho w}{\partial z} \tag{2}$$

where ρ is the density, t is the time and x, v and w are the velocity of flow in x, y and z directions.

$$\rho \frac{Dv}{Dt} = \rho g - \Delta P + \mu \Delta^2 \cdot v \tag{3}$$

Navier-Stokes equation can be expended into three equations to describe the flow motion in three coordinate system as in Equations (4)–(6).

$$\rho \frac{Du}{Dt} = \rho g_x - \frac{\partial p}{\partial x} + \mu \left(\frac{\partial^2 u}{\partial x^2} \right) + \frac{\partial^2 u}{\partial y^2} + \frac{\partial^2 u}{\partial z^2} \tag{4}$$

$$\rho \frac{Dv}{Dt} = \rho g_y - \frac{\partial p}{\partial y} + \mu \left(\frac{\partial^2 v}{\partial x^2} \right) + \frac{\partial^2 v}{\partial y^2} + \frac{\partial^2 v}{\partial z^2} \tag{5}$$

$$\rho \frac{Dw}{Dt} = \rho g_z - \frac{\partial p}{\partial z} + \mu \left(\frac{\partial^2 w}{\partial x^2} \right) + \frac{\partial^2 w}{\partial y^2} + \frac{\partial^2 w}{\partial z^2} \tag{6}$$

In Flow-3D each cell in the fluid domain has water volume fraction (F) ranging between 0 and 1. Where 1 represents cells that are fully occupied with water, while 0 represents cells that fully occupied with air. Values between 1 and 0 represent free surface between air and water as shown in Fig. 3. Flow-3D defines the free surface elevation by using the volume of fluid (VOF) function in Equation (7).

$$\frac{\partial F}{\partial t} + \frac{1}{V_F} \left[\frac{\partial}{\partial x} (FA_x u) + R \frac{\partial}{\partial y} (FA_y v) + \frac{\partial}{\partial z} (FA_z w) + \epsilon \frac{FA_x u}{x} \right] = F_{DIF} + F_{SOR} \tag{7}$$

where V_F is Volume of fluid fraction, F is the volume flow function, FSOR is the source function, A_x; A_y; A_z represent the fractional areas, u, v and

Table 1
Different experimental combinations.

Test	Q (m ³ /h)	S _o	v _{in} (m/s)	d _{in} (cm)
1	30	0.00	0.23	12.45
2	51.3	0.006	0.36	14.2
3	75.3	0.006	0.47	16.25
4	31	0.01	0.28	11.5

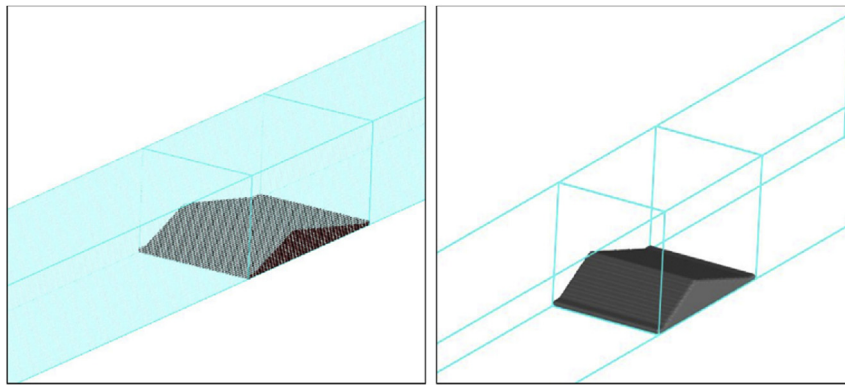


Fig. 4. Meshing and geometry after applying FAVOR solver of inside Flow-3D.

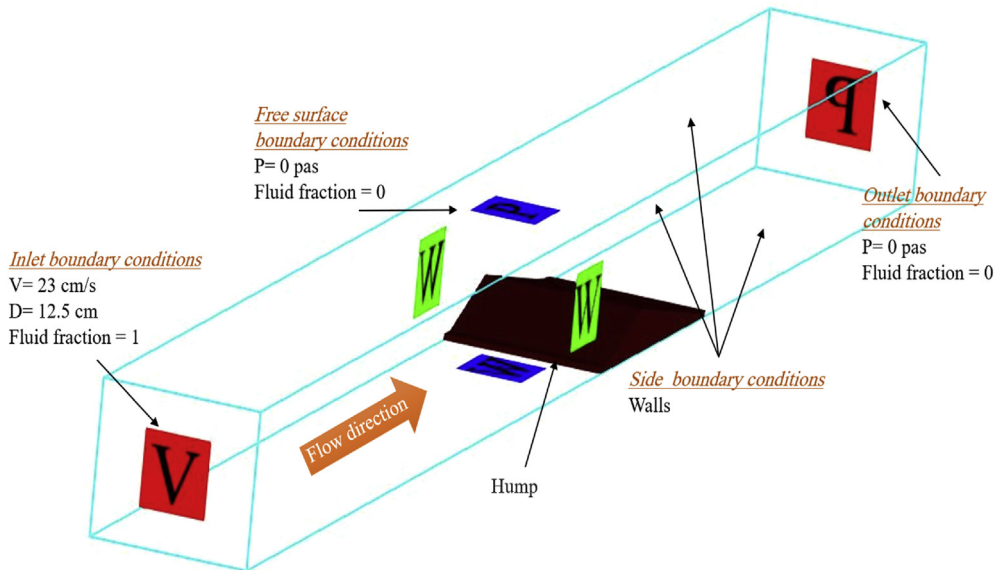


Fig. 5. Boundary conditions setting.

w are velocity components in x, y and z directions.

Materials and methods

A. Laboratory tests

Experiments were conducted in the hydraulic laboratory of Universiti Teknologi PETRONAS, Malaysia. A rectangular flume of 30 cm width 60 m height and 1000 cm length was used as shown in Fig. 1. A small hump with dimensions shown in Fig. 2 was placed and fixed inside the flume.

Also, water was supplied into the flume through a water pipe connected with storage tanks located underneath the flume. To reduce the flow turbulence at the entrance, some baffles were placed at the inlet (upstream) of the flume. During the experiments, point gauge was used to measure the water depths and flow meter (SEBA Hydrometer) was used to measure flow velocity at different locations, upstream and

Table 2
Mesh independency study.

Trail	Mesh size (cm)	Velocity (cm/s)	Cells number
1	1	113.7884	240,000
2	0.75	114.4713	563,640
3	0.5	115.0521	1,920,000
4	0.25	115.0473	15,360,000

downstream of the hump. Four cases of experiments with different flow discharges Q and bed slopes S_o were carried out as shown in Table 1.

The current meter used for velocity measurements recorded the number of rotations (p) for 30 s and the number of propeller rotation per second (n) was calculated using $n = p/30$. The velocities were computed using Equations (8) and (9) below:

$$v = 0.00123 + 0.2473(n) \quad \text{if } 0.00 < n < 1.74 \quad (8)$$

$$v = -0.0042 + 0.2568(n) \quad \text{if } 1.74 < n < 10 \quad (9)$$

Where v is the flow velocity (m/s) and n is the propeller rotation per second.

B. Numerical setup

In this study, the CFD commercialized code (Flow-3D) was used for numerical simulations. The software used the finite volume method (FVM) to solve mass, continuity and momentum conservation equations. Two phases (one fluid) with free surface flow was chosen and steady-state conditions of total mass, the average mean kinetic energy, the average mean turbulent energy and average mean turbulent dissipation with threshold variation of 1% were selected at the additional finishing time conditions.

3D Reynold Average Navier Stokes (RANS) equations were selected to solve turbulent flow. The fractional area volume obstacle representation

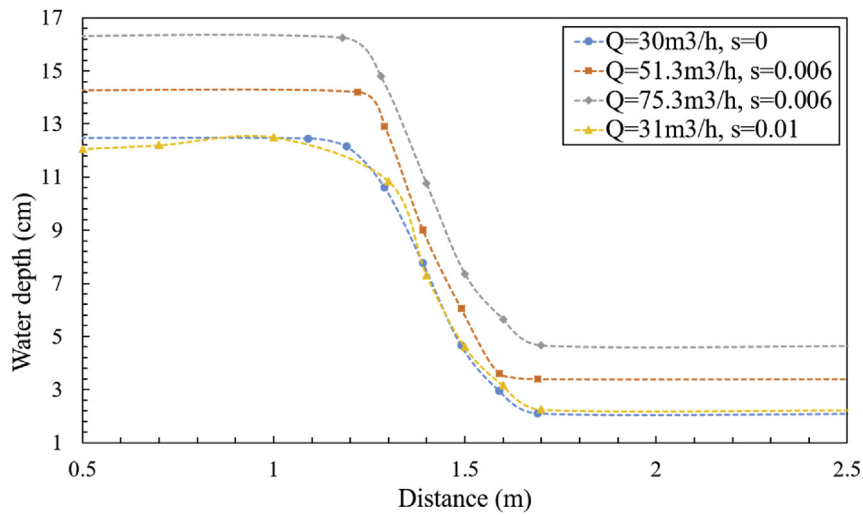


Fig. 6. Water flow profile (experimental results).

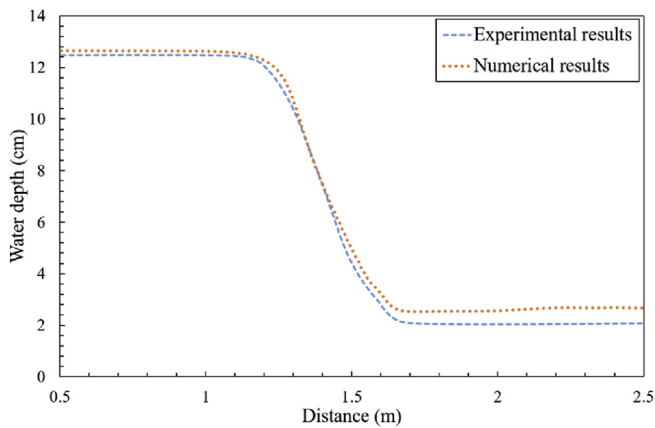


Fig. 7. Numerical vs experimental water profile case 1.

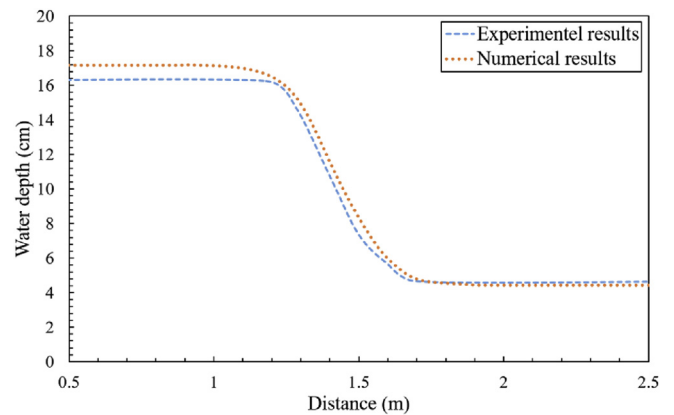


Fig. 9. Numerical vs experimental water profile case 3.

(FAVOR) method was used to define the effects of the meshing on the geometry. Hexahedral mesh blocks were defined for the simulations and the total number of mesh blocks were 1,920,000 cells. Fig. 4 shows the mesh and the geometry after applying FAVOR solver. The boundary conditions were defined with upstream inlet defined using flow velocity and flow depth, while downstream was defined as an outlet with 0 pressure. Also, channel bed and sides were defined as walls and the top surface as a free surface with 0 pressure and 0 fluid fractions as shown in Fig. 5.

4 history probes were located along the channel, 2 probes placed before the hump and the rest placed after the hump. These probes recorded hydraulic data including flow velocity, flow depth, Reynold's number, etc. Four cases were simulated with different flow discharges and bed slopes with an average simulation time of 6 h each. Mesh independency study has been conducted to find the accurate and suitable mesh size for this case. Depth average velocity veritable in case 1 at probe number 4 was selected to find the difference values at different mesh size as shown in Table 2.

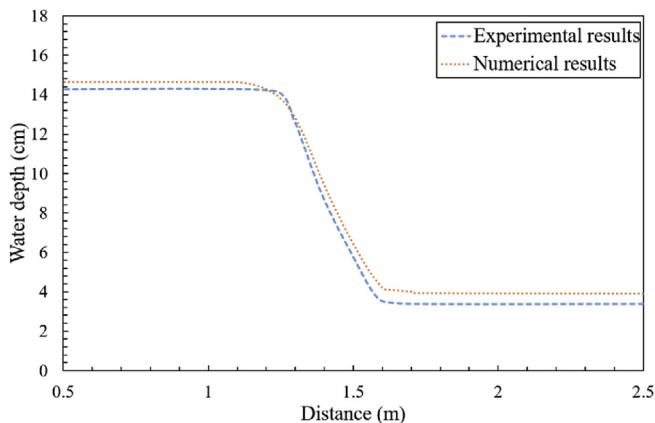


Fig. 8. Numerical vs experimental water profile case 2.

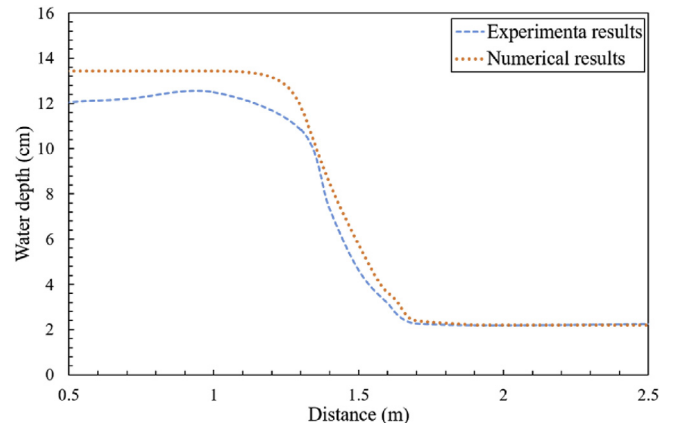


Fig. 10. Numerical vs experimental water profile case 4.

Table 3
Experimental and numerical depth average velocity variation for all cases.

Case	1		2		3		4	
	US	DS	US	DS	US	DS	US	DS
Numerical results	23.6	114	34.3	142	44.4	146	24.5	138
Experimental results	23.5	125	35	151	46.7	169	26.5	143

Table 4
Experimental and numerical froud's number variation for all cases.

Case	1		2		3		4	
	US	DS	US	DS	US	DS	US	DS
Numerical results	0.21	2.35	0.29	2.4	0.36	2.1	0.23	3
Experimental results	0.21	2.6	0.3	2.6	0.4	2.25	0.24	3.05

From Table 2 it can be noticed that the difference between trail number 3 and 4 in terms of velocity readings is not big, but in term of cells total number of cells is clear. This huge increasement in cells number required more time for execution. So, trail number 3 was selected to be the best mesh size for all cases during numerical simulation.

Results and discussion

In this study, the flow characteristics over a sharp-crested rectangular hump were analyzed using laboratory data and validated with numerical results. Fig. 6 show the water depth variation from upstream to downstream under four (4) cases of discharge variations (30, 51.3, 75.3 and 31 m³/h) and under the influence of three slopes of 0, 0.006 and 0.01. From the graphs, it can be observed that the water depth increase with an increase in discharge. The highest discharge stood at a depth of about 16.5 cm at the upstream and about 5.8 cm at the downstream. Negligible influence can be observed from the slope on the flow depth variations. The increase in the water depth was as a result of the presence of the hump which alters the flow pattern and hydraulic

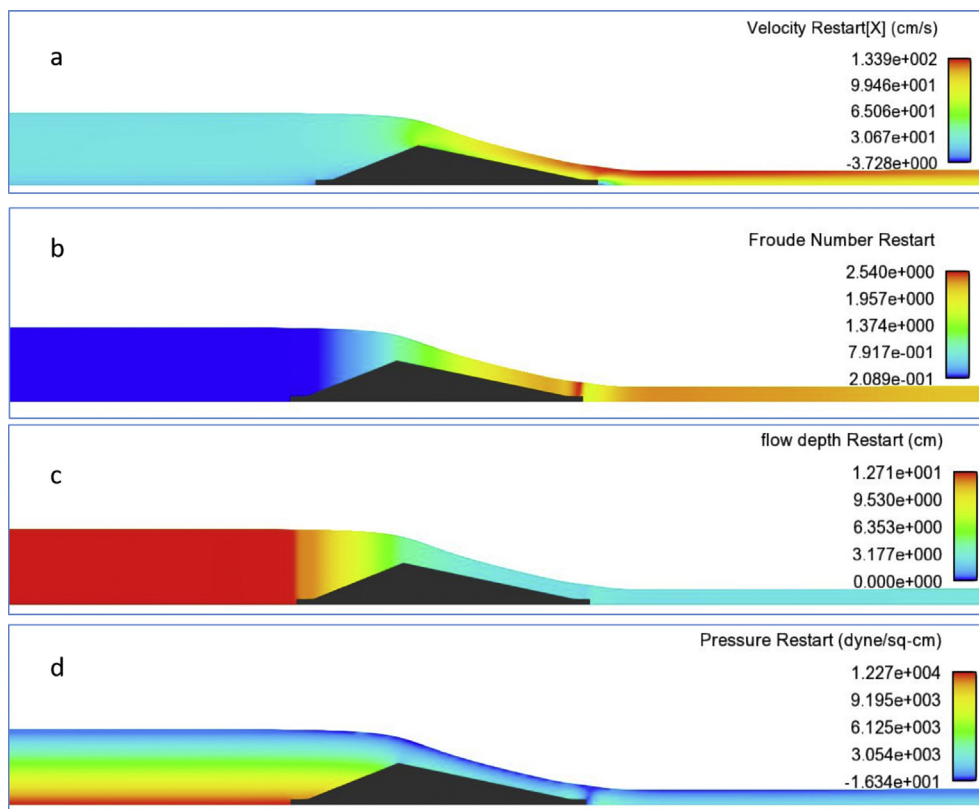


Fig. 11. a- Flow velocity variation contour b- Frauds number variation contour c- Flow depth variation contour d- Pressure variation contour.

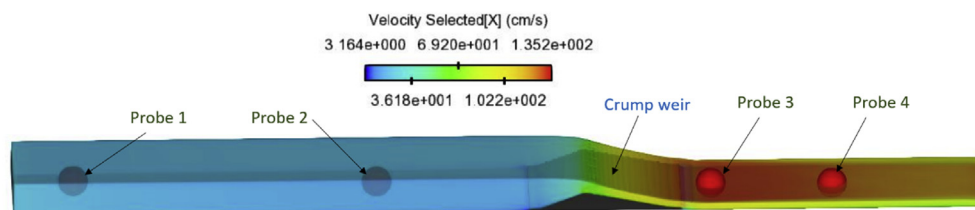


Fig. 12. 3-D flow velocity distribution and probes location.

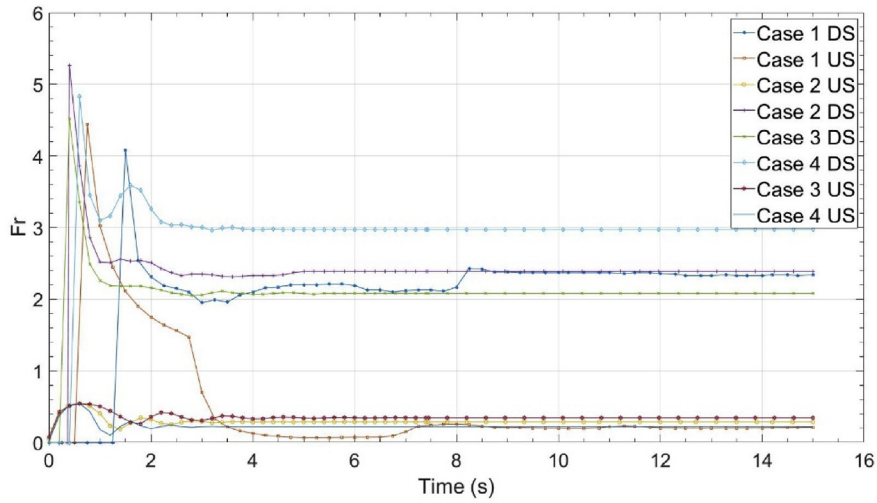


Fig. 13. Upstream and downstream Froude's number variation.

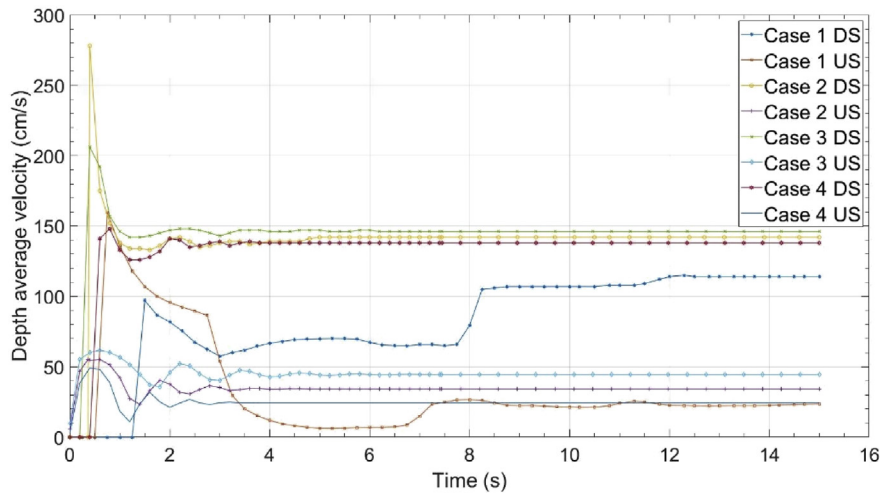


Fig. 14. Upstream and downstream depth average velocity variation.

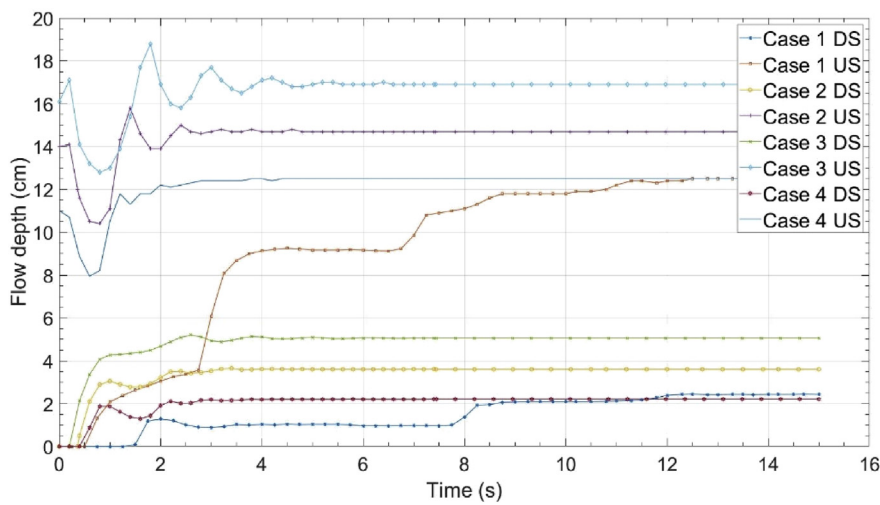


Fig. 15. Upstream and downstream flow depth variation.

characteristics. The smallest discharge (30 m³/h) can be observed to have the least water depth.

A. Validation of experimental results with numerical

In order to access the accuracy of the Flow 3D software, the compare between the numerical and experimental results, water surface profiles for all tested cases were extracted from the numerical simulation and plotted as shown in Figs. 7–10. From the graphs, a strong agreement can

be observed between the numerical and the experimental results as the variations fall between 4% and 5%. This variation is similar to the one in the study of [22] who observed variation between 1 and 3.5%.

Further, depth average velocity and Froude's number variables were extracted from the numerical simulation and compared with experiments results as shown in Tables 3 and 4. Good agreement between both results can be noticed at upstream (US) and downstream (DS) location.

B. Visualization of Flow Contours

In order to understand the physics of the velocity, Froude number, Flow depth and pressure variations in the flow with a hump, the contour plots were shown in Fig. 11. Fig. 11a show the variation of the flow velocity from upstream to downstream. It can be clearly observed that the flow has higher velocity at downstream than at the upstream this is because of the effect of the hump that generated more head pressure at the upstream side and less at the downstream side as shown in Fig. 11d. In addition, Fig. 11b shows the Froude's number variations from sub-critical to super-critical stage at the downstream with the highest value at the top of the right end of the hump. This is due to the geometry of the hump and nature of the transition points. Fig. 11c shows the flow depth variation between upstream and downstream of the hump. Further, a clearer 3D view of the flow velocity can be observed in Fig. 12 with the highest velocity at the downstream and lowest at the upstream because of the higher pressure created by the presence of the hump.

In addition, from the numerical results obtained using Flow 3D, the upstream and downstream variations in three parameters including Froude's number, flow velocity, and flow depth are as shown in Figs. 13–14 for all the four cases of discharges. From the figures, it can generally be observed that the flow at the upstream is sub-critical in nature with Froude's number values less than 1.0 while at the downstream the flows are supercritical with Froude's number values greater than 1.0 as in Fig. 13. Moreover, Flow velocity was found to generally increase as the flow moves from upstream to downstream in all the four cases as in Fig. 14. On the other hand, the flow depth was found to decrease from upstream to downstream for all the cases this is evident in Fig. 15.

Conclusions

This study modelled the flow characteristics over sharp crested triangular hump using numerical simulation and validated with experimental results. From the results and discussions, the following conclusions are drawn: Flow 3D software modelled flow characteristics through triangular hump with a greater degree of performance and accuracy. This is because strong agreement between the numerical and the experimental results was observed with minimum variations ranging between 4% and 5%. In terms of flow properties, it can be observed that the flows were sub-critical and supercritical in nature at the upstream and downstream respectively. This is ascribed to the presence of the hump along the flow path and can be highly applicable in the design of hydraulic structures especially in channel stabilization. In addition, flow velocities were found to generally increase as the flow moves from upstream to downstream in all the four cases (as seen in 2D and 3D views), while flow depths were found to decrease from upstream to downstream for all the cases. Overall, Flow 3D can be recommended as a useful tool to predict the behavior of weirs in discharge measurements, upstream and downstream flow stabilization. Moreover, performing similar modelling with

other turbulence models within the Flow 3D can be considered a strong scientific contribution to the field and is, therefore, highly recommended for future studies.

Conflict of interest

The authors declare no conflict of interest.

Acknowledgment

The authors acknowledge Universiti Teknologi PETRONAS, Malaysia for providing the enabling environment and hydraulic laboratory equipments to be utilized for this research and iRMC Bold2025, grant number RJO10436494, Universiti Tenaga Nasional, Malaysia.

References

- [1] R.L. France, *Wetland Design: Principles and Practices for Landscape Architects and Land-Use Planners*, WW Norton and Company, 2003.
- [2] A. Ferrari, SPH simulation of free surface flow over a sharp-crested weir, *Adv. Water Resour.* 33 (3) (2010) 270–276.
- [3] R. Singh, D. Manivannan, T. Satyanarayana, Discharge coefficient of rectangular side weirs, *J. Irrig. Drain. Eng.* 120 (4) (1994) 814–819.
- [4] S.M. Borghei, M.R. Jalili, M. Ghodsian, Discharge coefficient for sharp-crested side weir in subcritical flow, *J. Hydraul. Eng.* 125 (10) (1999) 1051–1056.
- [5] A. Al-Shukur, M. Al-jumaily, Z. Shaker, Experimental investigation of flow characteristics over crump weir with Different conditions, *Saudi J. Eng. Technol.* 2 (10) (2017) 373–379.
- [6] K.S. Erduran, G. Seckin, S. Kocaman, S. Atabay, 3D numerical modelling of flow around skewed bridge crossing, *Eng. Appl. Comput. Fluid Mech.* 6 (3) (2012) 475–489.
- [7] A.S.I. Abdurrahman, K.W. Yusof, H.B. Takaijudin, A. Ab, B.S. Iskandar, Effects of backwater on hydraulic performance evaluation of rainsmart modules in sustainable drainage systems, in: *International Conference on Water Resources*, Langkawi, Malaysia, November, 2018, pp. 27–28.
- [8] P.G. Chanele, J.C. Doering, Assessment of spillway modeling using computational uid dynamics, *Can. J. Civ. Eng.* 35 (12) (2008) 1481–1485.
- [9] S. Dehdar-Behbahani, A. Parsaie, Numerical modeling of flow pattern in dam spillways guide wall. Case study: balaroud dam, Iran, *Alexandria Eng. J.* 55 (1) (2016) 467–473.
- [10] A. Parsaie, A.H. Haghiabi, A. Moradinejad, CFD modeling of flow pattern in spillways approach channel, *Sustain. Water Resour. Manag.* 1 (3) (2015) 245–251.
- [11] H.K. Versteeg, W. Malalasekera, *An Introduction to Computational Fluid Dynamics: the infinite Volume Method*, Pearson education, 2007.
- [12] A.S.I. Abdurrahman, K.W. Yusof, H.B. Takaijudin, A.A. Ghani, M.M. Muhammad, A.T. Sholagberu, Advances and challenging issues in subsurface drainage module technology and BIOECODS: a review, in: *MATEC Web of Conferences*, 203, EDP Sciences, 2018, 07005.
- [13] S.Y. Kumcu, Investigation of flow over spillway modeling and comparison between experimental data and CFD analysis, *KSCCE J. Civil Eng.* 21 (3) (2017) 994–1003.
- [14] M. Darw, F. Moukalled, M. Luca, *Finite Volume Method in Computational Fluid Dynamics: an Advanced Introduction with OpenFOAM*, Springer, 2015.
- [15] H. Zahabi, M. Torabi, E. Alamatian, M. Bahiraei, M. Goodarzi, Effects of geometry and hydraulic characteristics of shallow reservoirs on sediment entrapment, *Water* 10 (12) (2018) 17–25.
- [16] G. Li, X. Li, J. Ning, Y. Deng, Numerical simulation and engineering application of a dovetail-shaped bucket, *Water* 11 (2) (2019) 242.
- [17] D.C. Lo, J.S. Liou, S. Chang, Hydrodynamic performances of air-water flows in gullies with and without swirl generation vanes for drainage systems of buildings, *Water* 7 (2) (2015) 679–696.
- [18] T. Cebeci, *Turbulence models and their application: efficient numerical methods with computer programs*, Springer Science and Business Media, 2003.
- [19] B. Mohammadi, O. Pironneau, *Analysis of the k-epsilon turbulence model*, 1993.
- [20] S. Patankar, *Numerical Heat Transfer and Fluid Flow*, CRC press, 1980.
- [21] L. Choufu, S. Abbasi, H. Pourshahbaz, P. Taghvaei, S. Tfwala, Investigation of flow, erosion, and sedimentation pattern around varied groynes under Different hydraulic and geometric conditions: a numerical study, *Water* 11 (2) (2019) 235.
- [22] S. Haun, N.R.B. Olsen, R. Feurich, Numerical modeling of flow over trapezoidal broad-crested weir, *Eng. Appl. Comput. Fluid Mech.* 5 (3) (2011) 397–405.